Navigating contradictions: Salmonella Typhimurium chemotactic responses to conflicting chemoeffector signals show parity with bacterial growth benefits

Zealon Gentry-Lear[1], Kailie Franco[2], Michael Shavlik[1], Michael J. Harms[1,3], and Arden Baylink[2*]

[1] University of Oregon, Department of Chemistry & Biochemistry, Eugene, OR, 97403
[2] Washington State University, Department of Veterinary Microbiology and Pathology, Pullman, WA 99164
[3] University of Oregon, Institute of Molecular Biology, Eugene, OR, 97403

[*] Corresponding author: arden.baylink@wsu.edu (A. Baylink)

Abstract

Many bacteria that colonize the guts of animals use chemotaxis to direct swimming motility and select sites for colonization based on sources of effectors derived from the host, diet, and microbial competitors of the local environ. The complex ecosystem of the gastrointestinal tract contains mixtures of chemoattractants and chemorepellents, but it remains poorly understood how swimming bacteria navigate conflicting signals. The enteric pathogen *Salmonella* Typhimurium possesses Tsr, a chemoreceptor protein that directs both chemoattraction and chemorepulsion responses, which we employed as a model to study chemotaxis in the presence of conflicting effector stimuli. We investigated how *S.* Typhimurium responds to human fecal matter, an effector source in the enteric lumen that contains high concentrations of indole, a bacteriostatic chemorepellent produced by the native commensals of the microbiota, and also nutrients such as L-serine, a chemoattractant. The indole concentration in human feces is more than 12-fold the concentration required for half-maximal chemorepulsion, however, we find *S.* Typhimurium, and various clinical isolates of non-typhoidal *S. enterica* serovars, are strongly attracted to liquid fecal matter. We further investigated the chemotactic responses of *S.* Typhimurium to titrations of indole and L-serine and revealed that chemorepulsion to indole is overridden in the presence of excess L-serine. We capture the inversion of these two opposing taxis behaviors in a phenomenon we define as "chemohalation" in which the bacteria organize into a halo around the treatment source with an interior zone of avoidance, which represents a compromise between chemoattraction and chemorepulsion. Growth analyses reveal that the chemotactic responses to these opposing effectors align chemoattraction and chemorepulsion with the relative growth of the bacteria in culture. Hence, our study supports the view that evolution has finely tuned chemotaxis to assess environmental habitability by evaluating the tradeoffs in bacterial growth based on the local combination of effectors.

Introduction

Bacteria that colonize the gastrointestinal tracts of humans and other animals must interpret a complex chemical landscape within the gut to locate preferred niches for colonization [1–4]. The intestinal lumen contains a variety of molecular cues that swimming bacteria use as information to promote attraction or repulsion from a colonization niche, reflecting possible growth advantages of the local environ [2,5]. Host-associated bacteria can interpret chemical signals including nutrients from the host diet, pH, inflammatory processes, and bacterial quorum signaling molecules—all of which may independently impact the growth and persistence of a bacterial population [6,7]. The role of these signals in directing bacterial localization is mostly understood in the context of an effector in isolation, i.e. whether bacteria swim towards or away from a specific chemical source. However, we lack an understanding of how bacteria navigate a complex landscape that contains mixtures of attractants and repellents, as in the host gut.

A widely conserved system by which bacteria survey their environment and control localization is chemotaxis, in which chemoreceptor proteins perceive exogenous ligands in the environment and regulate swimming motility to promote chemoattraction or chemorepulsion to sources of effectors (Fig. 1A) [1,2,7,8]. The chemotaxis systems of many host-associated bacteria, both native commensal and pathogenic species, have been shown to be important for colonization and survival within the host gut [1,4]. Chemotaxis enables motile bacteria to rapidly relocate based on novel sources of effector stimuli and to exert precise control of colonization at the micron-level scale [9–12]. These abilities translate into growth advantages during initial and long-term colonization because they allow bacteria to adapt to the dynamic circumstances within the gut, which changes frequently in terms of nutrient content, fluidic flow, and microbial competition [1,13,14]. Interestingly, a few chemoreceptors have been noted as directing both chemoattraction and chemorepulsion responses to discrete stimuli, suggesting that, in some cases, bacteria integrate conflicting signals into decisions on colonization at the single protein level [7,8,15]. One example is the chemoreceptor taxis to serine and repellents (Tsr), which we have shown to be widely distributed among bacterial colonizers of the gut, especially Enterobacteriaceae (Fig. 1A) [1,9].

A major factor in the population structure of gut bacteria is the host diet, which supplies high concentrations of energy-rich nutrients such as the amino acid L-serine (L-Ser) (Fig. 1B) [16,17]. Dietary nutrients are the subject of intense competition between microbes, which is one of the major barriers inhibiting the establishment of invading pathogens [18–21]. As microbiota consume dietary nutrients, they generate indole through the enzymatic activity of tryptophanases. Indole is an amphipathic chemical involved in interbacterial communication and known to have bacteriostatic and bactericidal properties [15,22–24]. Liquid human fecal matter contains indole in the range of 0.5-5 mM, and has been proposed to be a protective factor of the microbiota to inhibit invasion of enteric pathogens (Fig. 1B) [22,25–28] . The presence of both nutrients and toxins in dietary contents within the intestinal lumen would seem to provide a dilemma for bacteria in terms of knowing whether the growth benefit of the local nutrients outweighs the deleterious costs of indole (Fig. 1B). To better understand how bacteria employ chemotaxis to integrate conflicting signals into a course of navigation, we evaluated how a bacterial population responds to combinations of chemoattraction/nutrient and chemorepellent/toxin sources present in digested dietary material, and how this relates to bacterial growth. Using the enteric pathogen *Salmonella* Typhimurium as a model system, which employs Tsr in competing for nutrients with the microbiota during enteric infection, our study reveals that exposure to contradictory effector signals results in emergent behaviors not easily predicted from chemotactic responses to individual effectors [29,30]. These behaviors support an expanded lexicon for describing chemotactic responses and indicate further investigations into how bacteria navigate complex chemical landscapes are warranted to understand the roles of chemotaxis in organizing bacterial communities of the gut.

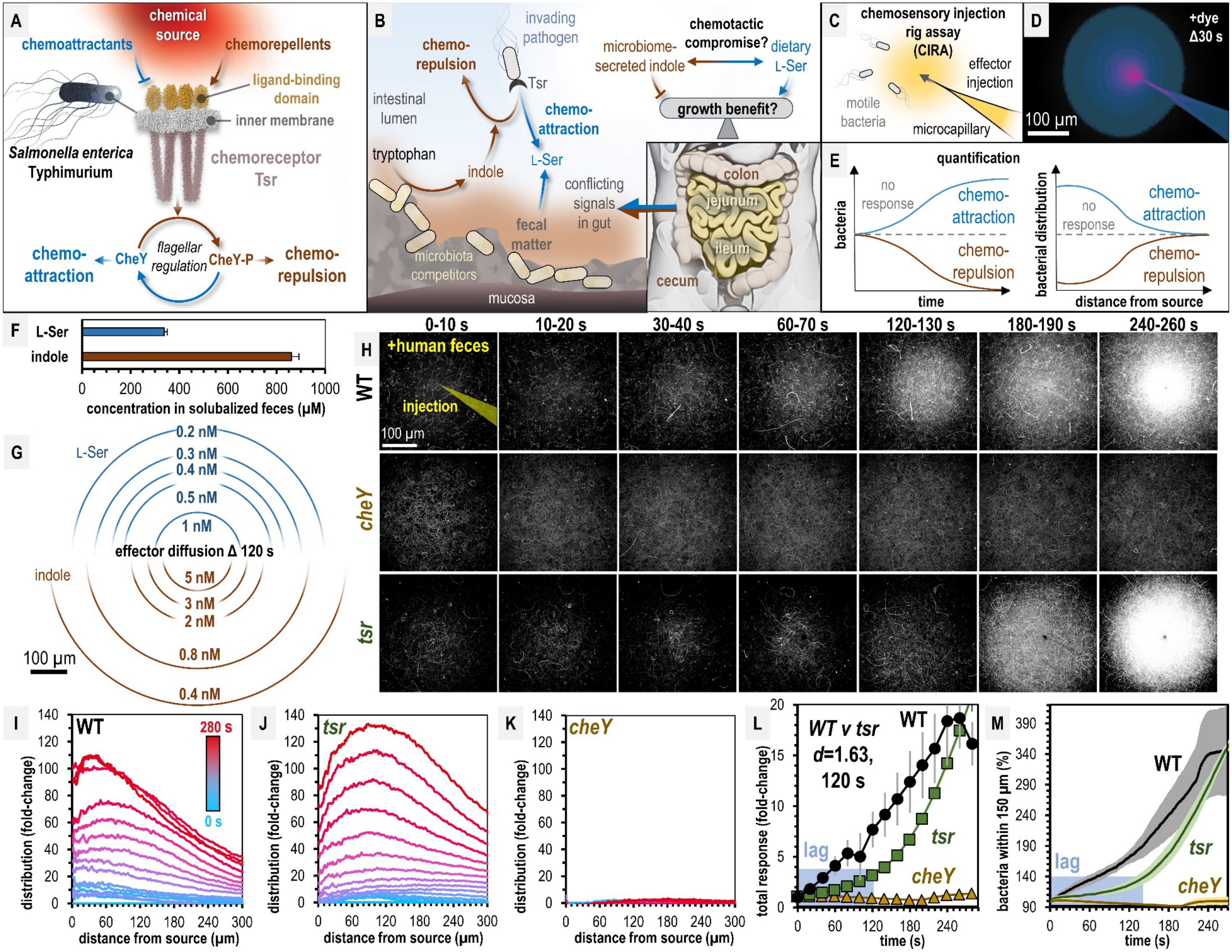
A
chemical source
chemoattractants
chemorepellents
ligand-binding domain
inner membrane
Salmonella enterica Typhimurium
chemoreceptor Tsr
flagellar regulation
chemo-attraction
CheY
CheY-P
chemo-repulsion
B
invading pathogen
chemo-repulsion
Tsr
intestinal lumen
chemo-attraction
tryptophan
indole
L-Ser
conflicting signals in gut
fecal matter
microbiota competitors
mucosa
chemotactic compromise?
microbiome-secreted indole
dietary L-Ser
growth benefit?
colon
jejunum
ileum
cecum
C
chemosensory injection rig assay (CIRA)
effector injection
motile bacteria
microcapillary
D
+dye Δ30 s
100 μm
E
quantification
bacteria
no response
chemo-attraction
chemo-repulsion
time
bacterial distribution
no response
chemo-attraction
chemo-repulsion
distance from source
F
L-Ser
indole
0
200
400
600
800
1000
concentration in solubalized feces (μM)
G
L-Ser
0.2 nM
0.3 nM
0.4 nM
0.5 nM
1 nM
effector diffusion Δ 120 s
indole
5 nM
3 nM
2 nM
0.8 nM
0.4 nM
100 μm
H
0-10 s
10-20 s
30-40 s
60-70 s
120-130 s
180-190 s
240-260 s
+human feces
WT
injection
100 μm
cheY
tsr
I
WT
280 s
0 s
distribution (fold-change)
0
20
40
60
80
100
120
140
0
60
120
180
240
300
distance from source (μm)
J
tsr
distribution (fold-change)
0
20
40
60
80
100
120
140
0
60
120
180
240
300
distance from source (μm)
K
cheY
distribution (fold-change)
0
20
40
60
80
100
120
140
0
60
120
180
240
300
distance from source (μm)
L
WT v tsr
d=1.63,
120 s
WT
tsr
cheY
lag
total response (fold-change)
0
5
10
15
20
0
60
120
180
240
time (s)
M
WT
tsr
cheY
lag
bacteria within 150 μm (%)
90
140
190
240
290
340
390
0
60
120
180
240
time (s)

Fig. 1. *Salmonella* Typhimurium exhibits attraction toward solubilized human feces. A-B. Overview of the role of Tsr in chemoattraction and chemorepulsion responses and premise of this study. C-E. CIRA experimental design and quantification. F-G. Quantification of total serine content (presumed to be nearly 100% L-Ser, see Methods) and indole in fecal treatments and diffusion modeling showing calculated local concentrations in CIRA experiments with feces. H. Max projections of representative *S.* Typhimurium IR715 responses to a source of solubilized human feces. See also Movie S1. I-K Mean bacterial distribution at 10 s intervals. L-M. Temporal analyses of area under the curve (AUC) or relative number of bacteria within 150 µm of the source. Effect size (Cohen's *d*) comparing responses of WT and *tsr* attraction at 120 s post-treatment is indicated. Data are means and error bars are standard error of the mean (SEM, n=3-5).

Results & Discussion

Non-typhoidal S. enterica exhibit attraction to human feces despite high indole content

Although indole is considered a chemorepellent for Enterobacteriaceae species, to the best of our knowledge no study has definitively shown whether these bacteria exhibit chemotactic responses to human fecal material, the primary biological source of indole in the enteric lumen [15,26–28,31,32]. To address this open question, we utilized a live-imaging approach we refer to as the chemosensory injection rig assay (CIRA) [33] to administer microscopic chemical treatments to motile bacteria and examine their responses to sources of effectors present in the gut. In this assay, a constant flow of approximately 300 femtoliters per minute is applied to inject the effector through a glass microcapillary 0.5 µm in diameter; chemoattraction is observed as an influx of cells into the field of view over time and congregation near the source, and chemorepulsion is observed as decreasing cells over time and avoidance of the central effector source (Fig. 1C-E) [9].

We first sought to examine the response of *S.* Typhimurium IR715 to a source of solubilized human fecal matter. Since the chemoreceptor Tsr plays a dominant role in *S.* Typhimurium chemotaxis and infection [29,30], we hypothesized that insight into the chemotactic behavior of this pathogen to the complex mixture of effectors in human feces could be gained by determining the concentration of two opposing singular effectors in the fecal material sensed through Tsr, the chemoattractant L-Ser and the chemorepellent indole. Unlike *Escherichia coli*, *S.* Typhimurium does not produce indole [34]. We determined the L-Ser and indole content of our solubilized human fecal samples to be 338 µM (+/- 11.7) and 862 µM (+/- 30), respectively (Fig.

1F, see Materials & Methods). We employed mathematical modeling of the diffusion of these effectors to calculate what local concentrations are experienced by the bacteria during CIRA experiments (Fig. 1G). These calculations indicate that at distances in the range of 50-300 µm from the treatment source, the local effector concentrations are in the nanomolar regime, with indole greater by about 3-fold over L-Ser (Fig. 1G). On the basis of the higher concentration of the repellent indole, we predicted a chemorepulsion response would occur when the bacteria were treated with solubilized human feces.

To test this idea, we compared the chemotactic behavior of wildtype (WT) *S.* Typhimurium and isogenic mutants *tsr*, which lacks the chemoreceptor Tsr but retains chemotaxis to other chemoeffectors, and *cheY*, which is motile but chemotaxis-null (Fig. 1H, Movie S1) [1]. Over the course of five minutes, we found that both WT and the *tsr* mutant exhibit strong chemoattraction to the fecal material, whereas the *cheY* mutant exhibits no chemotaxis response (Fig. 1H, Movie S1). When examining the radial distribution of the bacterial responses, we found that the WT more tightly centers around the treatment source, whereas the *tsr* mutant chemoattraction response is more diffuse and at late time points achieves a slightly greater magnitude (Fig. 1I-K, Movie S1). There also exists a temporal difference in the response between these two strains; we observed that the *tsr* strain experiences a lag compared to WT for 120 s that reduces the relative number of cells by about half at that timepoint (Fig. 1L-M, Movie S1). This came as a surprise, because we expected the *tsr* strain might have stronger chemoattraction to the fecal material given it is unable to perceive the chemorepellent indole. We wondered how this deficiency in fecal attraction might translate to direct competition, where strains are experiencing the same treatment source simultaneously. To address this, we performed CIRA with solubilized human feces and two strains present in the same pond, which we tracked independently through fluorescent markers (Fig. 2). As expected, WT shows a strong chemoattraction response versus *cheY*, the latter remaining randomly distributed (Fig. 2A). Interestingly, we found that when competed directly, WT vastly outperforms the *tsr* mutant, with the maximal bacterial distribution in proximity to the treatment source higher by about 4-fold (Fig. 2B). This supports that the chemoreceptor Tsr is involved in mediating taxis to human fecal matter.

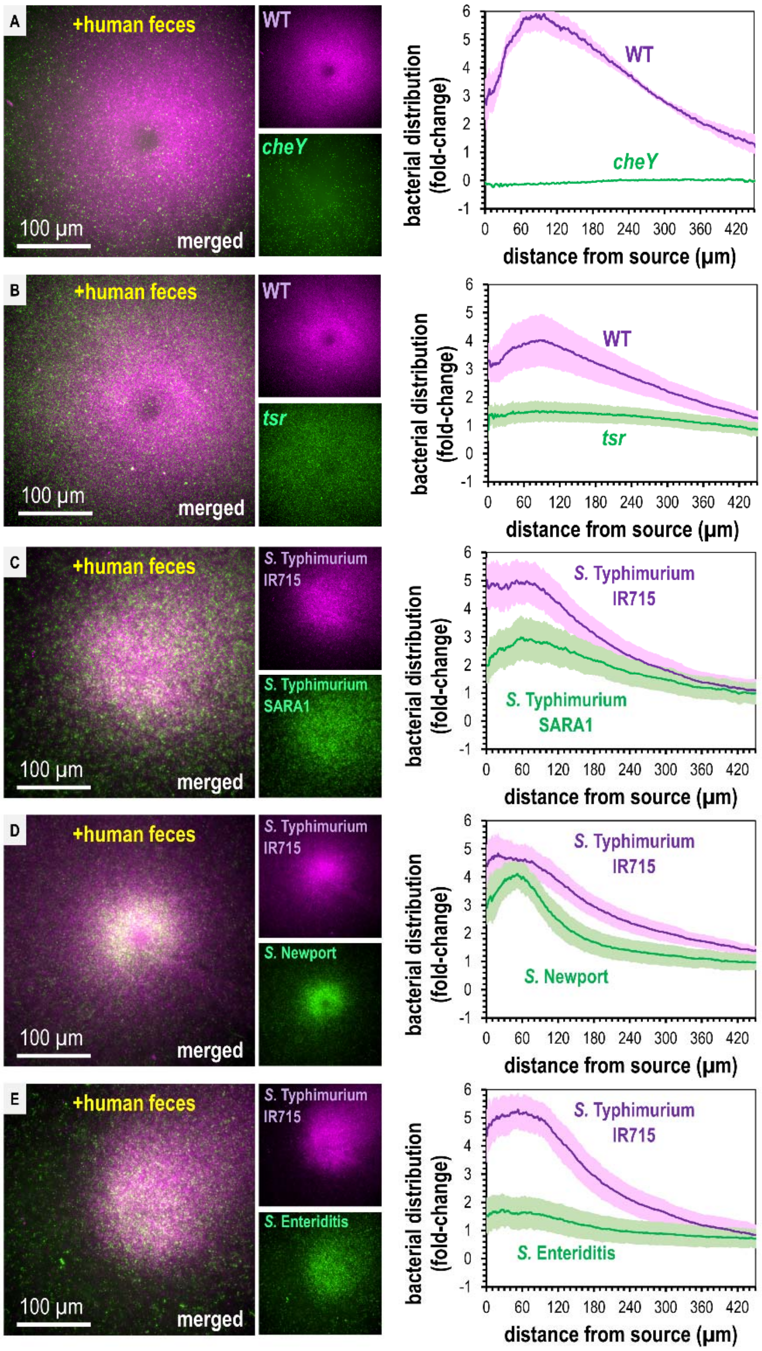

Fig. 2. Fecal attraction involves *cheY* and *tsr* and is conserved across clinical isolates and non-typhoidal *S. enterica* serovars. A-E. Dual-channel imaging of bacterial responses to solubilized human feces by WT *S.* Typhimurium IR715 (pink) and isogenic mutants or clinical isolate strains, as indicated. See also Movie S2. Data are means and error bars are standard error of the mean (SEM, n=3-5).

145 We were interested to learn whether diversity in fecal chemoattraction responses exist

across different *Salmonella* serovars, which differ in host specificity, and strains responsible for infections in humans, hypothesizing that some strains may exhibit chemorepulsion instead of chemoattraction. Using dual-channel imaging we competed *S.* Typhimurium IR715 with a clinical isolate of Typhimurium, SARA1, and found both strains exhibit fecal attraction, with SARA1 exhibiting a slightly diminished response (Fig. 2C, Movie S2). Next, we tested a clinical isolate of *S.* Newport, which has emerged as a common cause of salmonellosis in the United States and Europe [35,36], and found that this strain also exhibits fecal attraction with a tighter accumulation of cells at the treatment source compared to *S.* Typhimurium IR715 (Fig. 2D, Movie S2). Lastly, we examined the behavior of a drug-resistant clinical isolate of *S.* Enteriditis, a bacterium commonly transmitted zoonotically from poultry [36], and found this strain to exhibit weak fecal attraction (Fig. 2E, Movie S2). Thus, we identified no examples of indole chemorepulsion using the fecal biological source that contains the maximal indole *Salmonella* Typhimurium encounters *in vivo*, and found that taxis to fecal material is conserved across diverse non-typhoidal *Salmonella* serovars responsible for human infections.

Together, these data show that despite the high concentration of indole present in human fecal material, there are sufficient chemoattractants present to override a chemorepulsion response. Moreover, we did not observe evidence of bacterial killing on these short timescales, as might be predicted if indole was acting as a potent bactericidal agent against invading pathogens. We presume that the inhibited chemoattraction response of the *tsr* strain is a consequence of its inability to sense L-Ser present in the fecal matter, and that the chemoattraction response for that strain is driven by other chemoattractants, such as L-Asp and glucose, that are recognized through different chemoreceptors [1].

Mediation of opposing chemotactic responses by Tsr

Having identified Tsr as playing an important role in fecal attraction in the competition assays (Fig. 2B), we decided to further investigate how Tsr, as a single chemoreceptor, directs both chemoattraction and chemorepulsion responses to exogenous stimuli. Treatment with 5 mM purified L-Ser provokes a strong chemoattraction response and distinct reorganization of the bacterial population within 60 s (Fig. 3A). Treatment with 5 mM indole, a concentration at the upper end of what occurs in the human gut [28], induces rapid chemorepulsion with the bacteria vacating the region proximal to the source (Fig. 3B). Interestingly, the chemorepulsion response occurs more quickly than chemoattraction, with the

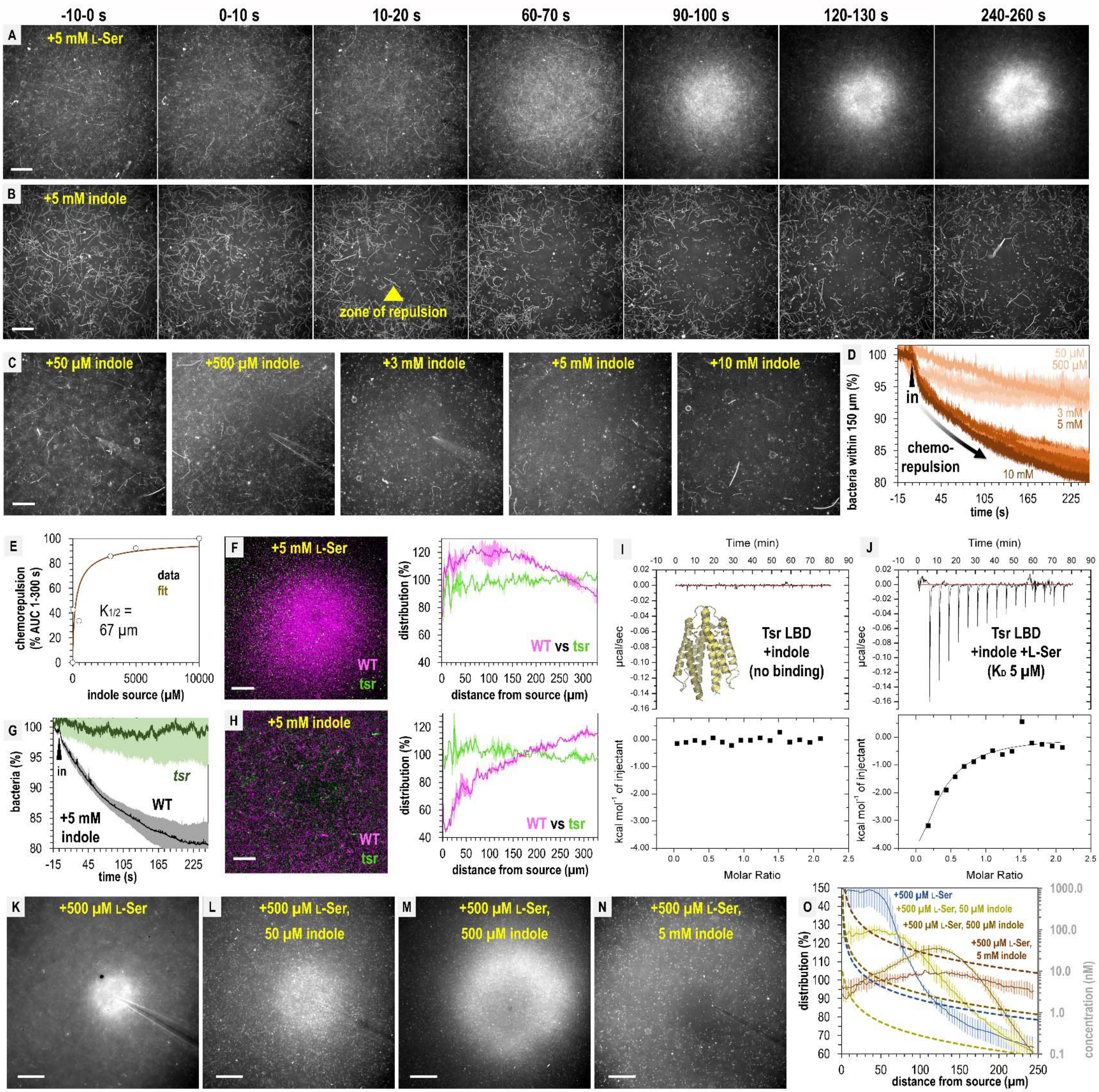
-10-0 s
0-10 s
10-20 s
60-70 s
90-100 s
120-130 s
240-260 s
A
+5 mM L-Ser
B
+5 mM indole
zone of repulsion
C
+50 µM indole
+500 µM indole
+3 mM indole
+5 mM indole
+10 mM indole
D
bacteria within 150 µm (%)
100
95
90
85
80
-15
45
105
165
225
time (s)
in
chemo-
repulsion
50 µM
500 µM
3 mM
5 mM
10 mM
E
chemorepulsion
(% AUC 1-300 s)
100
80
60
40
20
0
0
5000
10000
indole source (µM)
data
fit
K1/2 =
67 µm
F
+5 mM L-Ser
WT
tsr
distribution (%)
120
100
80
60
40
0
50
100
150
200
250
300
distance from source (µm)
WT vs tsr
G
bacteria (%)
100
95
90
85
80
-15
45
105
165
225
time (s)
in
tsr
WT
+5 mM
indole
H
+5 mM indole
WT
tsr
distribution (%)
120
100
80
60
40
0
50
100
150
200
250
300
distance from source (µm)
WT vs tsr
I
Time (min)
-10
0
10
20
30
40
50
60
70
80
90
µcal/sec
0.02
0.00
-0.02
-0.04
-0.06
-0.08
-0.10
-0.12
-0.14
-0.16
Tsr LBD
+indole
(no binding)
kcal mol-1 of injectant
0.00
-1.00
-2.00
-3.00
-4.00
0.0
0.5
1.0
1.5
2.0
2.5
Molar Ratio
J
Time (min)
-10
0
10
20
30
40
50
60
70
80
90
µcal/sec
0.02
0.00
-0.02
-0.04
-0.06
-0.08
-0.10
-0.12
-0.14
-0.16
Tsr LBD
+indole +L-Ser
(KD 5 µM)
kcal mol-1 of injectant
0.00
-1.00
-2.00
-3.00
-4.00
0.0
0.5
1.0
1.5
2.0
2.5
Molar Ratio
K
+500 µM L-Ser
L
+500 µM L-Ser,
50 µM indole
M
+500 µM L-Ser,
500 µM indole
N
+500 µM L-Ser,
5 mM indole
O
distribution (%)
150
140
130
120
110
100
90
80
70
60
0
50
100
150
200
250
distance from source (µm)
concentration (nM)
1000.0
100.0
10.0
1.0
0.1
+500 µM L-Ser
+500 µM L-Ser, 50 µM indole
+500 µM L-Ser, 500 µM indole
+500 µM L-Ser,
5 mM indole

Fig. 3. Chemotactic compromise orchestrated by Tsr in response to conflicting effector signals. A-B. Representative max projections of *S.* Typhimurium IR715 response to sources of L-Ser or indole. C. Representative responses at 300 s of indole treatment. D-E. Quantification of chemorepulsion as a function of indole concentration (n=3-5). F-H. Comparison of WT and *tsr* mutant responses to L-Ser or indole. I-J. Isothermal titration calorimetry (ITC) experiments with 50 µM *S.* Typhimurium Tsr ligand-binding domain (LBD) and indole, or with L-Ser in the presence of 500 µM indole (see Methods). K-N. Representative max projections of responses to treatments of L-Ser and indole, as indicated. O. Relative bacterial distribution in response to treatments with the mean value normalized to 100%. Diffusion modeling of local effector concentrations based on sources of 5 mM indole (dark brown), 500 µM L-Ser (blue), 500 µM indole (light brown), and 50 µM indole (yellow) are shown as dashed lines plotted with the secondary gray y-axis. Data are means and error bars are standard error of the mean (SEM, n=3-5). AUC indicates area under the curve. Scale bars are 100 µm.

zone of repulsion clearly visible within the first 10 s of indole exposure (Fig. 3B). A prior study suggested that bacteria can adapt rapidly to indole and, under some circumstances, exhibit chemoattraction [15,24]. To understand the temporal dynamics of the chemorepulsion response, and identify the effective source concentration that drives indole chemorepulsion, we performed a titration of indole across five concentrations spanning 50 µM to 10 mM (Fig. 3C). At all concentrations tested, indole induced chemorepulsion responses and the bacteria avoided the treatment source for the full duration of the 5-minute experiment (Fig. 3C-D). At source concentrations exceeding 3 mM essentially all motile cells vacate the field of view within 60 s. Integrating these chemorepulsion response curves and fitting them to a Monad curve suggests an indole source concentration of approximately 67 µM is sufficient for half-maximal ($K_{1/2}$) chemorepulsion (Fig. 3E). These data show that even though we observe a strong chemoattraction response to fecal material, the major biological source of indole in the gut, indole is indeed a potent chemorepellent for *S.* Typhimurium.

Although Tsr is recognized as a sensor of L-Ser, the literature is conflicting as to whether this chemoreceptor is required for indole chemorepulsion. Much of the prior work addressing this question does not measure chemotaxis directly, i.e. actual migration of bacteria in response to a source of indole, but extrapolates how bacteria will organize based on measurements of flagellar rotation bias in a bath of indole [24,37]. A study by Yang and colleagues reports that chemoreceptors Tsr and Tar both respond to indole, and that indole can regulate chemotaxis independent of chemoreceptors [15]. This study quantified cell attachment to an agar plug containing indole, but did not investigate the temporal dynamics nor the behavior of the non-attached population [15]. To address whether Tsr in *Salmonella* mediates the indole chemorepulsion response we observe, we compared responses of the WT or *tsr* mutant to a source of indole using CIRA. These data show the *tsr* mutant to fully lack indole chemorepulsion (Fig. 3G). This demonstrates that indole chemotaxis under these conditions is chemoreceptor-dependent, requiring Tsr, and presumably CheY, to control the localization of the bacteria in response to a source of indole. We next performed competition assays between WT and *tsr* with L-Ser (Fig. 3F), or indole (Fig. 3H), and found that the *tsr* mutant is unable to respond to either effector. Since our earlier work demonstrated that the *tsr* strain retains chemotaxis to other stimuli [9] we conclude that Tsr is responsible for indole chemorepulsion.

The molecular mechanism of Tsr-mediated chemorepulsion from indole remains unknown. It could occur through a direct interaction or reflect the responsiveness of Tsr to perturbations in the proton motive force [15]. The Tsr protein consists of a cytosolic coiled-coil region that interfaces with the histidine kinase chemotaxis protein A (CheA), a membrane-spanning HAMP domain, and a periplasmic ligand-binding domain (LBD) that binds L-Ser [9,38]. The crystal structure of the *S.* Typhimurium Tsr LBD clearly defines how the binding site recognizes the L-Ser ligand (PDB code: 8fyv), and we thought it unlikely indole can be accommodated at the same site [9]. Nevertheless, to test whether the Tsr LBD binds indole directly, we expressed and purified the LBD, corresponding to the soluble portion located in the periplasm, and performed isothermal titration calorimetry (ITC). These data show no binding occurs between the Tsr LBD and indole (Fig. 3I). We next wondered if indole is an allosteric regulator of the Tsr LBD, possibly through interacting with the L-Ser bound form or interfering with L-Ser recognition. To address these possibilities, we performed ITC of 50 µM Tsr LBD with L-Ser in the presence of 500 µM indole, and observed a robust exothermic binding curve and K_D of 5 µM, identical to the binding of L-Ser alone (Fig. 3J) [9]. These data indicate indole does not alter the Tsr LBD affinity for L-Ser. We conclude that Tsr senses indole either through an indirect mechanism or through interaction at a site other than the periplasmic LBD.

Striking compromise through chemohalation

Having characterized Tsr as responsible for both chemorepulsion from indole and chemoattraction to L-Ser, we sought to learn how the bacterial population behaves when confronted with a combination of these effectors, as in the human gut. Potentially, in the presence of both effectors, one signal could dominate the chemotactic response. Alternatively, the behavior could shift between chemoattraction and chemorepulsion in a concentration-dependent manner. To address this question, we performed CIRA with 500 µM L-Ser, which elicits a strong chemoattraction response, and compared chemotaxis behaviors when the chemoattractant versus chemorepellent effector ratio is shifted to be 10:1, 1:1, or 1:10, all concentrations being within the range of what *S.* Typhimurium encounters *in vivo* (Fig. 3K-N).

These experiments reveal a fascinating transition in the distribution of the bacterial population as a function of increasing chemorepellent (Fig. 3K-O). When only the chemoattractant is present, the bacterial population organizes tightly around the L-Ser source (Fig. 3K). When indole is introduced at a concentration 10-fold lower than that of L-Ser, the bacterial distribution retains its chemoattraction character, but the population becomes more diffuse and less tightly associated with the treatment source (Fig. 3L). At a 1:1 ratio of chemoattractant and chemorepellent a new behavior emerges in which the bacterial population forms a halo with a peak approximately 125 µm from the treatment source (Fig. 3M). This behavior appears to be an intermediate response between chemoattraction and chemorepulsion and is not well-described by either term. Within the entire field of view there is an increase in total number of cells (which might traditionally be referred to as chemoattraction), but in the range of 0-50 µm the bacterial distribution is much lower, approximately the same as the baseline of the experiment start (Fig. 3M). To our knowledge, no prior work has defined a term for this response, so here we have chosen to refer to it as "chemohalation" in reference to the halo structure formed by the cells around the treatment source.

Chemohalation represents a compromise in positional location, at the population level, between the chemoattraction driven by L-Ser and the chemorepulsion driven by indole. When the concentration of indole is 10-fold higher than L-Ser the bacteria exhibit diffuse chemohalation with a wide zone of avoidance (0-100 µm) and a small peak near 125 µm (Fig. 3N). Interestingly, this demonstrates that even at the highest concentration of indole *S.* Typhimurium might encounter in the gut, the presence of a chemoattractant can override indole chemorepulsion. Whereas 5 mM indole on its own induces a strong chemorepulsion response (Fig. 3B), the addition of 10-fold lower L-Ser effectively converts the behavior to a null response, where the bacteria show little bias in their distribution as a function of the chemoeffector source (Fig. 3N). Or, put another way, a 10-fold higher concentration of chemorepellent is sufficient to nullify the strong chemoattraction response to L-Ser.

We were surprised that the most distinct chemohalation response we observed was for indole and L-Ser at equal concentration (Fig. 3M). These two effectors have similar diffusion coefficients and so their relative concentration should remain similar as they diffuse outward from the source. We wondered why, then, the population selects discrete zones for avoidance versus accumulation (Fig. 3O). We hypothesized the transition between chemoattraction, chemohalation, and chemorepulsion might be better understood by calculating the local concentrations of effectors experienced by the cells, which suggests that 10 nM indole is a threshold for behavioral change when cells encounter mixtures of indole and L-Ser (Fig. 3O). Where the local indole concentration exceeds 10 nM, repulsion dominates, either eliciting chemorepulsion, if indole is the sole effector, or, when in combination with L-Ser, promoting the zone of avoidance in the interior of the chemohalation halo (Fig. 3O). The distance from the effector source at which the local indole concentration falls below 10 nM correspond, roughly, with the peak of chemohalation where cells accumulate (Fig. 3O). This suggests that *S.* Typhimurium's chemotactic signaling priority switches from indole to L-Ser in a gradual, concentration-dependent manner, with chemohalation representing a snapshot near the threshold for this switch where the opposing effectors are near equal ratio. (Fig. 3K-O).

Chemotactic responses reflect potential for growth benefits

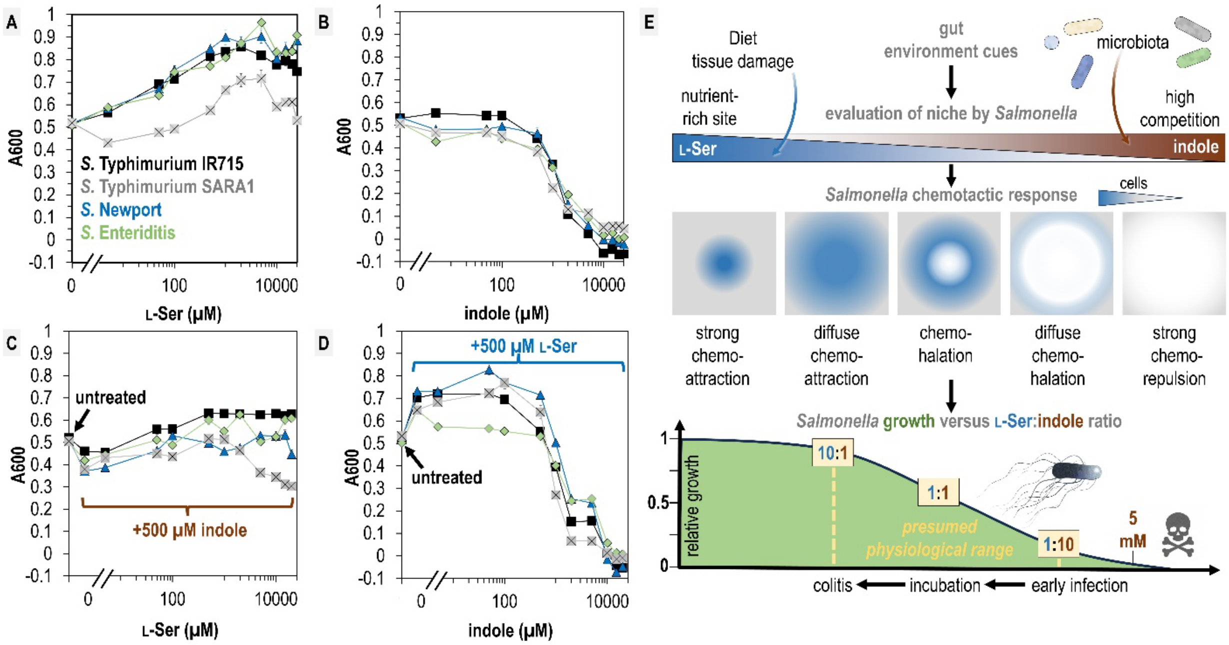

The robust attraction of diverse non-typhoidal *Salmonella* strains to human fecal matter, a biological source of the chemorepellent indole, was striking and suggests that the behavior of bacteria in complex biological settings may not be accurately captured by single effector interactions (Movie S2). Despite this, we questioned whether a reductionist approach could still offer insights into understanding why bacteria are attracted to a biological solution with high concentrations of indole, which is known for its inhibition of bacterial growth. Operating on the assumption that chemotaxis functions to achieve growth advantages for the bacterial population [2,14], we examined how the growth of these strains are affected by 0-25 mM indole or L-Ser in a background of minimal media (MM). As expected, increasing amounts of the nutrient L-Ser provide a growth advantage for all *Salmonella* strains analyzed, with maximal benefit achieved by approximately 500 µM (Fig. 4A). Equivalent treatments with indole show tolerance up to approximately 1 mM, with growth inhibition occurring in the range of 1-5 mM, and lethality occurring at indole concentrations greater than 5 mM (Fig. 4B). Thus, the chemotactic response of *S.* Typhimurium to these effectors relates to their propensity to enhance or inhibit growth.

Having seen how bacterial growth is impacted by each effector independently, we next examined bacterial growth when treated with 500 µM of one effector, and increasing concentrations of the second effector. We selected this concentration based on being sufficient to induce a small, but measurable, growth change (increased growth for L-Ser addition, decreased for indole), being in the same concentration regime as our solubilized human fecal treatments

(Fig. 1F), and reflecting the source concentrations used in our chemotaxis analyses. Even though the direct impact on growth of the primary effector was minimal, the pattern of growth upon addition of the second effector was markedly different (Fig. 4C-D). Addition of L-Ser in a background of 500 µM indole provides only a small growth enhancement (Fig. 4C), substantially diminished compared to treatments with L-Ser alone (Fig. 4A). Interestingly, addition of 500 µM L-Ser increases tolerance for indole up to about 1 mM, above which indole toxicity is unavoidable (Fig. 4D). Thus, we find that physiologically relevant combinations of indole and L-Ser that elicit chemotactic responses also alter *Salmonella* growth, and that there appears to be a non-additive trade-off between the benefits from nutrient acquisition versus cost of growth inhibition from indole.

A working model relating chemotactic behaviors to environ growth potential

Fig. 4. Non-typhoidal *S. enterica* growth in the presence of indole and L-Ser. A-B. Bacterial growth as a function of L-Ser or indole, at the time point where the untreated culture reaches A600 of 0.5. C-D. Bacterial growth +/- treatment with 500 µM indole or L-Ser, and increasing concentrations of indole or L-Ser, as indicated. Data are means and error bars are standard error of the mean (SEM, n=8-24). E. Working model for how Tsr orchestrates bacterial localization, through chemotaxis, to achieve growth benefits when faced with a mixture of nutrients (L-Ser) and bactericides (indole).

Bacteria inhabiting the human gastrointestinal tract regularly encounter complex chemical environments containing both chemoattractants and chemorepellents. However, the evaluation of microbial chemosensing responses to effectors is often conducted in isolation from biological and ecological contexts, potentially leading to an over- or underemphasis on specific interactions. This discrepancy is evident in our model system, where *S. enterica* perceives indole as a chemorepellent, but when exposed to human feces—the primary source of indole in the human gut—the bacteria exhibit a robust chemoattraction response. This unexpected behavior arises due to the presence of numerous chemoattractant signals that overpower the chemorepulsion response (Fig. 1, Fig. 2, Movie S1, Movie S2). We anticipate that these responses may vary depending on factors such as the nutrient composition of the diet, microbiome activity, and the health of the host.

Our data suggest some insight into bacterial chemotaxis to biological solutions can be gained through examining responses to physiologically relevant mixtures of the major chemoattractants and chemorepellents. In the model system we have investigated here, *S. enterica* uses the single chemoreceptor Tsr to orchestrate a compromise in positional location when faced with physiologically relevant concentrations of the chemorepellent indole and chemoattractant L-Ser, effectors present at high concentration in human fecal material. The bacteria adopt discrete localization patterns based on the ratio of chemoattractant versus chemorepellent, with chemohalation occurring when the ratio of these signals nears 1:1 (Fig. 4E). Based on diffusion modeling of the microgradient, we expect that the local concentration that triggers the chemotactic response to be on the nanomolar scale, two orders of magnitude lower than the source concentration, and far below what we found to impact growth (Fig. 3O). This presumably allows the bacteria to survey the effector sources at a safe distance to assess the growth potential of a niche before committing to colonization and sessility. Our observation that supplementing *S. enterica* with L-Ser substantially increases tolerance to indole implies that the robust chemoattraction of these bacteria to fecal treatments reflects their assessment that the abundance of nutrients, including L-Ser, outweighs the growth costs associated with indole.

Our study suggests that further investigations into how bacterial chemosensing operates to make decisions on localization when faced with conflicting signals will be useful for understanding the roles of these systems *in vivo*. Whether chemohalation serves a specific growth advantage, or is simply an artifact of opposing responses operating simultaneously, remains to be determined. An analogous example of chemohalation is found in a prior study involving the gastric pathogen *Helicobacter pylori* responding to urea (a chemoattractant) and hydrochloric acid (a chemorepellent)—conflicting signals encountered in the human stomach [10]. It is interesting to note that, in the case of *Salmonella* and indole, the chemorepellent response, despite being more rapid, is rather easily overridden by the presence of chemoattractants. In the context of this study, this may reflect that the cells are in fact well-prepared to tolerate indole if they have sufficient nutrients available. It remains unclear if conditions within the human gut exist where indole excreted from the microbiota will elicit the strong chemorepulsion response seen to purified indole *in vitro*. Considering that indole only impairs *Salmonella* growth at concentrations significantly higher than those inducing chemorepulsion, indole may be more aptly thought of as a molecular cue that signals the presence of microbial competitors, an unfavorable colonization dynamic, rather than merely a toxin. We propose that in a host landscape comprising numerous microniches, the dual functions of Tsr aid *Salmonella* in selecting the best compromise between abundant nutrients, signaled by local L-Ser, and low competition, signaled by local indole.

Materials and Methods

RESOURCE AVAILABILITY

Lead contact

Further information and requests for resources and reagents should be directed to and will be fulfilled by the lead contact, Arden Baylink (arden.baylink@wsu.edu).

Materials availability

Strains and plasmids generated in this study will be made available upon request by the Lead Contact with a completed Materials Transfer Agreement.

Data availability

Source data from this work are archived and available upon request by the Lead Contact.

EXPERIMENTAL MODEL AND SUBJECT DETAILS

Bacterial strains

Bacterial strains and plasmids used in this study are listed in Table S1. As previously described [9], bacteria intended for chemotaxis assays were grown overnight in tryptone broth (TB) with antibiotic selection, as appropriate. Motile bacteria were prepared with a 1:1000 back-dilution and grown shaking for approximately 4 hours at 30° C or 37° C, as indicated, to reach A_{600} of 0.5. Cells were centrifuged, washed, and resuspended in a chemotaxis buffer (CB) containing 10 mM potassium phosphate (pH 7), 10 mM sodium lactate, and 100 μM EDTA to A_{600} of 0.2 and rocked gently at room temperature until fully motile. For *in vitro* growth analyses, cultures were grown overnight in Luria-Bertani (LB) media at 37° C. Subsequently, 5 µl of A_{600} 2.0 cells were used to inoculate 200 µl of minimal media (MM), containing 47 mM Na_2HPO_4, 22 mM KH_2PO_4, 8 mM NaCl, 2mM $MgSO_4$, 0.4% glucose (w/v) 11.35 mM $(NH_4)_2SO_4$, 100 μM $CaCl_2$ and L-Ser and/or indole at the described concentrations, and cultured in a 96-well microtiter plate. Cultures were grown at 37˚ C and monitored by A_{600} readings at 5-minute intervals.

METHOD DETAILS

Chemosensory injection rig assay (CIRA)

CIRA was performed as described previously [9]. Briefly, an Eppendorf Femtotip 2 microcapillary containing the treatment of interest was lowered into a pond of 50 µl of motile cells using a Sutter micromanipulator. An injection flow of effector into the pond approximately of 300 fl per minute was achieved using a Femtojet 4i set to P_c 35. Solubilized fecal treatments were prepared by dissolving 1 g of commercially-obtained human feces (Innovative Research) in 10 ml of CB. The solution was clarified by centrifugation at 10,000 g for 20 minutes followed by sterile filtration through a 0.2 µm filter. Treatment solutions of indole and L-Ser were also diluted into CB and sterile filtered before application. Videos were recorded using an inverted Nikon Ti2 microscope with heated sample chamber at 37 ˚C. Modeling of the microgradient generated through CIRA was performed as described earlier [9], based on the continual injection and diffusion of an effector from a fixed point source.

Purification of recombinant Salmonella Typhimurium Tsr LBD

Purification of *Salmonella* Typhimurium Tsr LBD was performed as described previously [9]. Rosetta BL21(DE3) *E. coli* cells with a Tsr-LBD-pet-30a(+) vector were grown with LB and 20 µg kanamycin and induced at A600 of 0.8 with 0.4 mM isopropyl β-D-1-thiogalactopyranoside (IPTG). Cells were harvested after 3 H of growth at 37˚ C. Cells were lysed, the lysate was clarified through centrifuged, and the soluble fraction was subjected to an ammonium sulfate precipitation, with Tsr LBD precipitating in the 20-40% fraction. The fractions were pooled, treated with TEV protease to remove the N-terminal expression sequence, and further purified using an anion exchange column and Akta FPLC. Lastly, the protein was purified by gel filtration using an S200 column with a final buffer of 50 mM Tris pH 7.5, 1 mM EDTA, and 150mM NaCl and stored at 7 mg/ml at -80 C.

Isothermal titration calorimetry ligand binding studies (ITC)

ITC experiments were performed using a Microcal ITC200 instrument (GE Healthcare). Either 500 μM indole or L-Ser was titrated in 2.5 μL injections into a 200 μL sample cell containing 50 μM Tsr LBD. For the indole/L-Ser competition experiment, 500 μM indole was added to both the titrant and sample cell, thus providing a constant excess background concentration of indole. For all experimental conditions, blank titrations were also collected in which indole or L-Ser was titrated into a cell containing buffer alone. All experiments were performed using thoroughly degassed samples at 25 °C in 50 mM Tris, 150 mM NaCl, 1 mM EDTA, pH 7.5. The reference power was set to 5 μcal/sec. The resulting power curves were integrated using the Origin analysis software included with the instrument. The heat of dilution was subtracted from each point using the blank. A single-site binding model was then fit to the data, floating parameters describing the binding enthalpy (ΔH), equilibrium constant (K_D), and apparent binding stoichiometry (n). The instrument software was used for this purpose.

Quantification of indole and serine in human fecal samples

Solubilized human feces was prepared as described above for CIRA, and analyzed by mass spectrometry to determine the molar serine content as a service through the University of Washington Mass Spectrometry Center. This measurement reflects total serine, of which close to 100% is expected to be L-Ser [39]. Indole content of solubilized human fecal treatments was determined as described in earlier work using a hydroxylamine-based calorimetric assay using purified indole as a reference [25].

QUANTIFICATION AND STATISTICAL ANALYSIS

Quantification of CIRA data

Videos of chemotactic responses were quantified as described previously [9]. The number of cells in each frame was calculated through determining a ratio of fluorescence intensity per cell for frames pre-treatment, and extrapolated using the ‘plot profile’ function of ImageJ. The distribution of the bacterial distribution was calculated using the Radial Profile ImageJ plugin.

Statistical Analyses

Effect sizes for data are indicated with Cohen's *d* value:

$$\mathrm{d} = \frac{\mathrm{M}_1 - \mathrm{M}_2}{\sigma_{\mathrm{pooled}}}$$

where:

$$\sigma_{pooled} = \sqrt{\frac{{\sigma_1}^2 + {\sigma_2}^2}{2}}$$

Acknowledgements

Funding for this research was provided by NIAID through awards 1K99AI148587 and 4R00AI148587-03, and funding from Washington State University to AB. Bacterial strains were provided by Nikki Shariat (University of Georgia, Athens), Nkuchia Mikanatha and Pennsylvania NARMS and GenomeTrakr Programs, and Andreas Bäumler (University of California, Davis). All research on human samples was performed in accordance with, and approval of, the Institutional Biosafety Committee at Washington State University.

Author Contributions

A.B. conducted the CIRA experiments. Z.G. performed growth curve analyses. K.F. performed the microgradient modeling. M.S. and M.J.H. performed the ITC experiments. All authors contributed to data analyses and writing of the manuscript.

Declaration of Interests

A.B. owns Amethyst Antimicrobials, LLC.

References

1. Zhou, B., Szymanski, C. M. & Baylink, A. Bacterial chemotaxis in human diseases. *Trends in Microbiology* (2022) doi:10.1016/j.tim.2022.10.007.
2. Keegstra, J. M., Carrara, F. & Stocker, R. The ecological roles of bacterial chemotaxis. *Nat Rev Microbiol* 1–14 (2022) doi:10.1038/s41579-022-00709-w.

3. Bi, S. & Sourjik, V. Stimulus sensing and signal processing in bacterial chemotaxis. *Current Opinion in Microbiology* **45**, 22–29 (2018).

4. Matilla, M. A. & Krell, T. The effect of bacterial chemotaxis on host infection and pathogenicity. *FEMS Microbiol Rev* **42**, (2018).

5. Waite, A. J., Frankel, N. W. & Emonet, T. Behavioral Variability and Phenotypic Diversity in Bacterial Chemotaxis. *Annu. Rev. Biophys.* **47**, 595–616 (2018).

6. Bi, S. & Lai, L. Bacterial chemoreceptors and chemoeffectors. *Cell. Mol. Life Sci.* **72**, 691–708 (2015).

7. Matilla, M. A. & Krell, T. Chemoreceptor-based signal sensing. *Current Opinion in Biotechnology* **45**, 8–14 (2017).

8. Ortega, Á., Zhulin, I. B. & Krell, T. Sensory Repertoire of Bacterial Chemoreceptors. *Microbiology and Molecular Biology Reviews* **81**, e00033-17 (2017).

9. Glenn, S. J. *et al.* Bacterial vampirism mediated through chemotaxis. *bioRxiv* 2023.07.07.548164 (2023) doi:10.1101/2023.07.07.548164.

10. Huang, J. Y., Sweeney, E. G., Guillemin, K. & Amieva, M. R. Multiple Acid Sensors Control Helicobacter pylori Colonization of the Stomach. *PLOS Pathogens* **13**, e1006118 (2017).

11. Perkins, A., Tudorica, D. A., Amieva, M. R., Remington, S. J. & Guillemin, K. Helicobacter pylori senses bleach (HOCl) as a chemoattractant using a cytosolic chemoreceptor. *PLoS Biol* **17**, e3000395 (2019).

12. Huang, J. Y. *et al.* Chemodetection and Destruction of Host Urea Allows Helicobacter pylori to Locate the Epithelium. *Cell Host Microbe* **18**, 147–156 (2015).

13. Keilberg, D., Zavros, Y., Shepherd, B., Salama, N. R. & Ottemann, K. M. Spatial and Temporal Shifts in Bacterial Biogeography and Gland Occupation during the Development of a Chronic Infection. *mBio* **7**, e01705-16.

14. Matilla, M. A., Gavira, J. A. & Krell, T. Accessing nutrients as the primary benefit arising from chemotaxis. *Current Opinion in Microbiology* **75**, 102358 (2023).

15. Yang, J. *et al.* Biphasic chemotaxis of Escherichia coli to the microbiota metabolite indole. *PNAS* **117**, 6114–6120 (2020).

16. Kitamoto, S. *et al.* Dietary L-serine confers a competitive fitness advantage to Enterobacteriaceae in the inflamed gut. *Nat Microbiol* **5**, 116–125 (2020).

17. Sugihara, K. & Kamada, N. 10 THE ROLE OF DIETARY L-SERINE IN THE REGULATION OF INTESTINAL MUCUS BARRIER DURING INFLAMMATION. *Gastroenterology* **158**, S70 (2020).

18. Rogers, A. W. L., Tsolis, R. M. & Bäumler, A. J. Salmonella versus the Microbiome. *Microbiology and Molecular Biology Reviews* **85**, e00027-19 (2020).

19. Ruddle, S. J., Massis, L. M., Cutter, A. C. & Monack, D. M. Salmonella-liberated dietary L-arabinose promotes expansion in superspreaders. *Cell Host & Microbe* **31**, 405-417.e5 (2023).

20. Panwar, R. B., Sequeira, R. P. & Clarke, T. B. Microbiota-mediated protection against antibiotic-resistant pathogens. *Genes Immun* **22**, 255–267 (2021).

21. Sugihara, K. *et al.* Mucolytic bacteria license pathobionts to acquire host-derived nutrients during dietary nutrient restriction. *Cell Reports* **40**, 111093 (2022).

22. Li, X., Zhang, B., Hu, Y. & Zhao, Y. New Insights Into Gut-Bacteria-Derived Indole and Its Derivatives in Intestinal and Liver Diseases. *Frontiers in Pharmacology* **12**, (2021).

23. Lee, J.-H. & Lee, J. Indole as an intercellular signal in microbial communities. *FEMS Microbiology Reviews* **34**, 426–444 (2010).

24. Gupta, R. *et al.* Indole modulates cooperative protein–protein interactions in the flagellar motor. *PNAS Nexus* **1**, pgac035 (2022).

25. Darkoh, C., Chappell, C., Gonzales, C. & Okhuysen, P. A Rapid and Specific Method for the Detection of Indole in Complex Biological Samples. *Appl Environ Microbiol* **81**, 8093–8097 (2015).

26. Chappell, C. L. *et al.* Fecal Indole as a Biomarker of Susceptibility to Cryptosporidium Infection. *Infect Immun* **84**, 2299–2306 (2016).

27. Ye, X. *et al.* Dual Role of Indoles Derived From Intestinal Microbiota on Human Health. *Front Immunol* **13**, 903526 (2022).

28. Kumar, A. & Sperandio, V. Indole Signaling at the Host-Microbiota-Pathogen Interface. *mBio* **10**, e01031-19 (2019).

29. Rivera-Chávez, F. *et al.* Energy Taxis toward Host-Derived Nitrate Supports a Salmonella Pathogenicity Island 1-Independent Mechanism of Invasion. *mBio* **7**, e00960-16 (2016).

30. Rivera-Chávez, F. *et al.* Salmonella uses energy taxis to benefit from intestinal inflammation. *PLoS Pathog* **9**, e1003267 (2013).

31. Bansal, T. *et al.* Differential Effects of Epinephrine, Norepinephrine, and Indole on Escherichia coli O157:H7 Chemotaxis, Colonization, and Gene Expression. *Infection and Immunity* **75**, 4597–4607 (2007).

32. Kohli, N. *et al.* The microbiota metabolite indole inhibits Salmonella virulence: Involvement of the PhoPQ two-component system. *PLOS ONE* **13**, e0190613 (2018).

33. Glenn, S. J. *et al.* Human Serum is a Potent Chemoattractant for Enterobacteriaceae Species Associated with Gastrointestinal Bleeding. *eLife* **12**, (2023).

34. Nikaido, E. *et al.* Effects of indole on drug resistance and virulence of Salmonella enterica serovar Typhimurium revealed by genome-wide analyses. *Gut Pathog* **4**, 5 (2012).

35. Shariat, N. *et al.* Subtyping of Salmonella enterica Serovar Newport Outbreak Isolates by CRISPR-MVLST and Determination of the Relationship between CRISPR-MVLST and PFGE Results. *J Clin Microbiol* **51**, 2328–2336 (2013).

36. Ferrari, R. G. *et al.* Worldwide Epidemiology of Salmonella Serovars in Animal-Based Foods: a Meta-analysis. *Appl Environ Microbiol* **85**, e00591-19 (2019).

37. Montrone, M., Oesterhelt, D. & Marwan, W. Phosphorylation-independent bacterial chemoresponses correlate with changes in the cytoplasmic level of fumarate. *J Bacteriol* **178**, 6882–6887 (1996).

38. Cassidy, C. K. *et al.* Structure and dynamics of the E. coli chemotaxis core signaling complex by cryo-electron tomography and molecular simulations. *Commun Biol* **3**, 1–10 (2020).

39. Nakade, Y. *et al.* Gut microbiota–derived D-serine protects against acute kidney injury. *JCI Insight* **3**, e97957.

40. Beltran, P. *et al.* Reference collection of strains of the Salmonella typhimurium complex from natural populations. *Microbiology* **137**, 601–606 (1991).

41. Shariat, N. *et al.* The combination of CRISPR-MVLST and PFGE provides increased discriminatory power for differentiating human clinical isolates of Salmonella enterica subsp. enterica serovar Enteritidis. *Food Microbiology* **34**, 164–173 (2013).

42. Wiles, T. J. *et al.* Modernized Tools for Streamlined Genetic Manipulation and Comparative Study of Wild and Diverse Proteobacterial Lineages. *mBio* **9**, e01877-18 (2018).

Supplementary Information

Supplementary Movies

Movie S1. Chemotactic response of *S.* Typhimurium IR715 to solubilized human feces. Representative CIRA experiments showing *S.* Typhimurium IR715 WT and mutant strains responding to a source of liquid human feces (shown at 10x speed) Viewable at: https://www.youtube.com/watch?v=BqUcRN3YwjU

Movie S2. Chemotactic response of *S.* enterica clinical isolates to solubilized human feces. Representative CIRA experiments showing competition between *S.* Typhimurium IR715 (mplum) and clinical isolates, as indicated (gfp), responding to a source of solubilized human feces Viewable at: https://www.youtube.com/watch?v=dLsFDV0XgpY

Supplementary Tables

Table S1. Bacterial strains and plasmids used in this study.

Strain/plasmid	Description	Source
S. enterica Typhimurium		
IR715	Nalidixic acid-derivative of ATCC 14028	[30]
FR13	IR715 *cheY*::Tn*10* (Tet^R)	[30]
FR4	IR715 tsr::pFR3 (Tet^R)	[30]
SARA1	Isolated from patient in Mexico	[40]
S. enterica Newport		
M11018046001A	Isolated from patient in PA, USA	[35]
S. enterica Enteriditis		
05E01375	Isolated from patient in PA, USA	[41]

E. coli K12	Rosetta(DE3) BL21 derivative	Millipore Sigma
Plasmids		
pXS-sfGFP	pGEN-mcs with a modular sfGFP expression scaffold (Amp^R)	[42]
pXS-mPlum	pGEN-mcs with a modular mPlum expression scaffold (Amp^R)	[42]
pET-30a(+)-*Se*TsrLBD	Vector for recombinant expression of *Se*Tsr LBD (Kan^R)	[9]

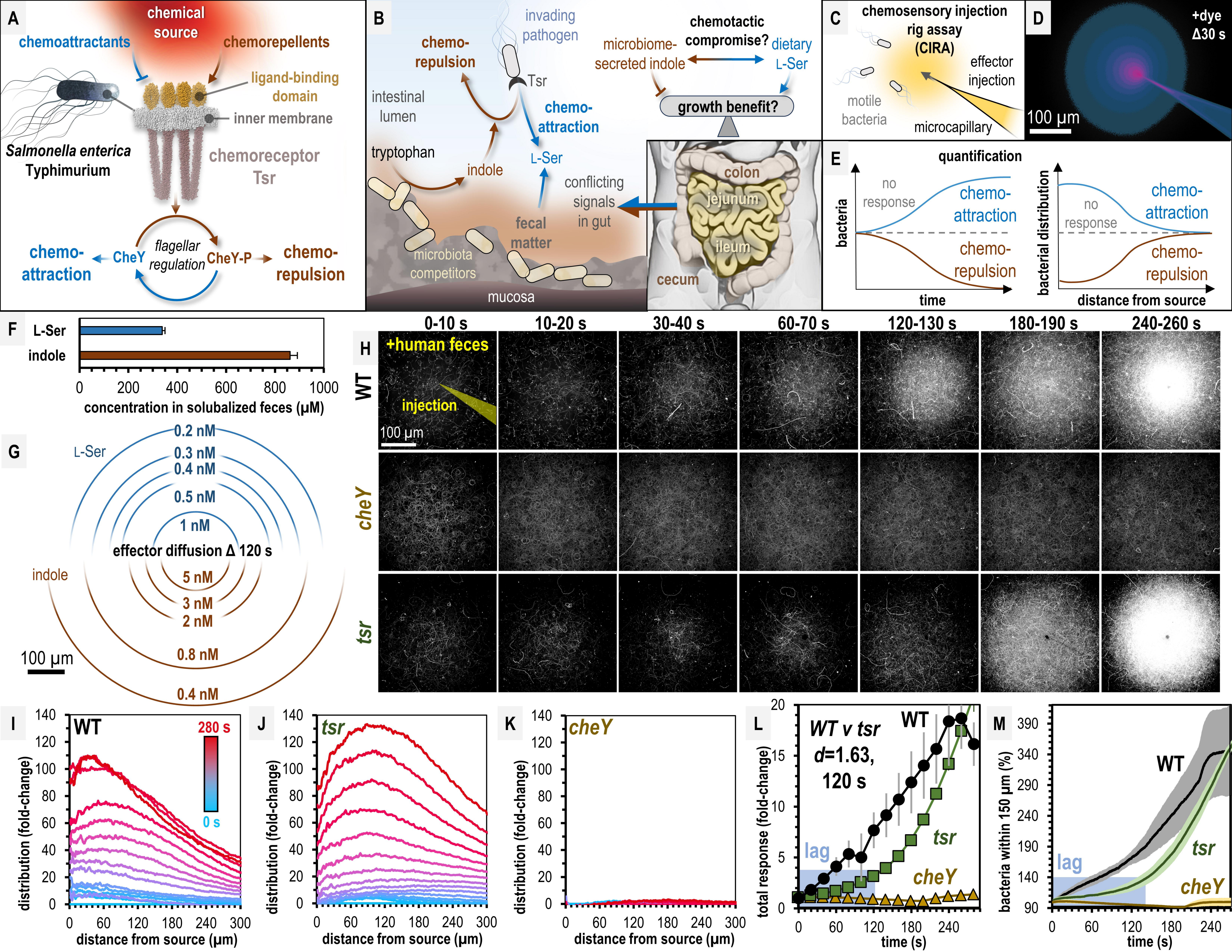
A
chemical source
chemoattractants
chemorepellents
ligand-binding domain
inner membrane
Salmonella enterica Typhimurium
chemoreceptor Tsr
flagellar regulation
CheY
CheY-P
chemo-attraction
chemo-repulsion
B
invading pathogen
chemo-repulsion
Tsr
intestinal lumen
chemo-attraction
tryptophan
indole
L-Ser
conflicting signals in gut
fecal matter
microbiota competitors
mucosa
chemotactic compromise?
microbiome-secreted indole
dietary L-Ser
growth benefit?
colon
jejunum
ileum
cecum
C
chemosensory injection rig assay (CIRA)
effector injection
motile bacteria
microcapillary
D
+dye Δ30 s
100 µm
E
quantification
bacteria
no response
chemo-attraction
chemo-repulsion
time
bacterial distribution
distance from source
F
L-Ser
indole
0
200
400
600
800
1000
concentration in solubalized feces (µM)
G
L-Ser
0.2 nM
0.3 nM
0.4 nM
0.5 nM
1 nM
effector diffusion Δ 120 s
5 nM
3 nM
2 nM
0.8 nM
0.4 nM
indole
100 µm
H
0-10 s
10-20 s
30-40 s
60-70 s
120-130 s
180-190 s
240-260 s
+human feces
WT
injection
100 µm
cheY
tsr
I
WT
280 s
0 s
distribution (fold-change)
distance from source (µm)
J
tsr
K
cheY
0
20
40
60
80
100
120
140
0
60
120
180
240
300
L
WT v tsr
d=1.63, 120 s
WT
tsr
cheY
lag
total response (fold-change)
0
5
10
15
20
time (s)
M
WT
tsr
cheY
lag
bacteria within 150 µm (%)
90
140
190
240
290
340
390

A
+human feces
100 µm
merged
WT
cheY
bacterial distribution (fold-change)
distance from source (µm)
-1
0
1
2
3
4
5
6
0
60
120
180
240
300
360
420
WT
cheY
B
+human feces
100 µm
merged
WT
tsr
bacterial distribution (fold-change)
distance from source (µm)
WT
tsr
C
+human feces
100 µm
merged
S. Typhimurium IR715
S. Typhimurium SARA1
bacterial distribution (fold-change)
distance from source (µm)
S. Typhimurium IR715
S. Typhimurium SARA1
D
+human feces
100 µm
merged
S. Typhimurium IR715
S. Newport
bacterial distribution (fold-change)
distance from source (µm)
S. Typhimurium IR715
S. Newport
E
+human feces
100 µm
merged
S. Typhimurium IR715
S. Enteriditis
bacterial distribution (fold-change)
distance from source (µm)
S. Typhimurium IR715
S. Enteriditis

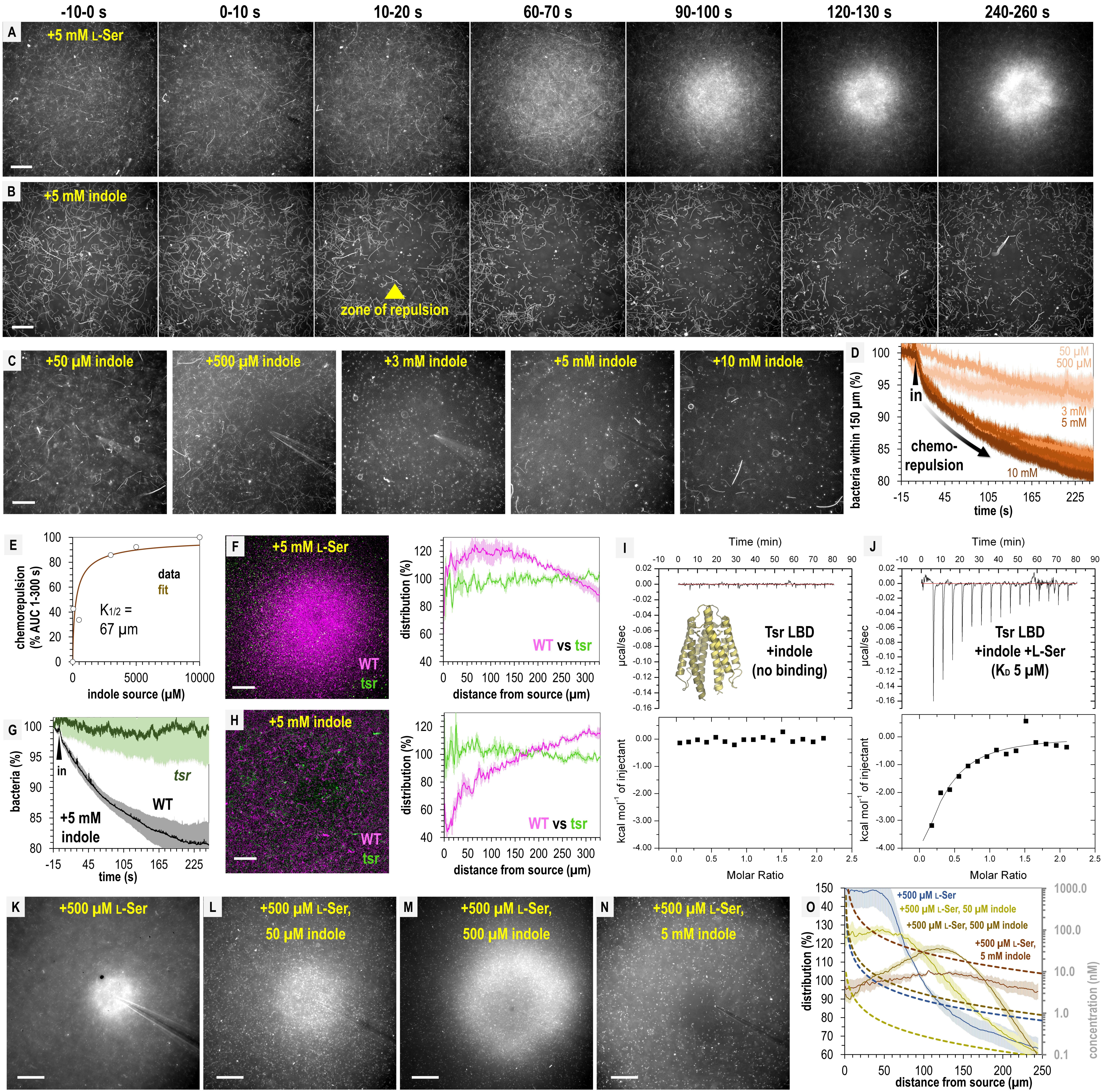
-10-0 s
0-10 s
10-20 s
60-70 s
90-100 s
120-130 s
240-260 s
A
+5 mM L-Ser
B
+5 mM indole
zone of repulsion
C
+50 µM indole
+500 µM indole
+3 mM indole
+5 mM indole
+10 mM indole
D
bacteria within 150 µm (%)
100
95
90
85
80
-15
45
105
165
225
time (s)
in
chemo-
repulsion
50 µM
500 µM
3 mM
5 mM
10 mM
E
chemorepulsion (% AUC 1-300 s)
100
80
60
40
20
0
5000
10000
indole source (µM)
data
fit
K1/2 =
67 µm
F
+5 mM L-Ser
WT
tsr
distribution (%)
120
100
80
60
40
0
50
100
150
200
250
300
distance from source (µm)
WT vs tsr
G
bacteria (%)
in
tsr
WT
+5 mM
indole
time (s)
H
+5 mM indole
WT
tsr
distribution (%)
distance from source (µm)
WT vs tsr
I
Time (min)
-10
0
10
20
30
40
50
60
70
80
90
µcal/sec
0.02
0.00
-0.02
-0.04
-0.06
-0.08
-0.10
-0.12
-0.14
-0.16
Tsr LBD
+indole
(no binding)
kcal mol⁻¹ of injectant
0.00
-1.00
-2.00
-3.00
-4.00
0.0
0.5
1.0
1.5
2.0
2.5
Molar Ratio
J
Time (min)
µcal/sec
Tsr LBD
+indole +L-Ser
(KD 5 µM)
kcal mol⁻¹ of injectant
Molar Ratio
K
+500 µM L-Ser
L
+500 µM L-Ser,
50 µM indole
M
+500 µM L-Ser,
500 µM indole
N
+500 µM L-Ser,
5 mM indole
O
distribution (%)
150
140
130
120
110
100
90
80
70
60
+500 µM L-Ser
+500 µM L-Ser, 50 µM indole
+500 µM L-Ser, 500 µM indole
+500 µM L-Ser,
5 mM indole
1000.0
100.0
10.0
1.0
0.1
concentration (nM)
0
50
100
150
200
250
distance from source (µm)

A
1
0.9
0.8
0.7
0.6
0.5
0.4
0.3
0.2
0.1
0
-0.1
A600
S. Typhimurium IR715
S. Typhimurium SARA1
S. Newport
S. Enteriditis
0
100
10000
L-Ser (µM)
B
A600
0
100
10000
indole (µM)
C
untreated
+500 µM indole
A600
0
100
10000
L-Ser (µM)
D
+500 µM L-Ser
untreated
A600
0
100
10000
indole (µM)
E
Diet
tissue damage
gut
environment cues
microbiota
nutrient-
rich site
evaluation of niche by Salmonella
high
competition
L-Ser
indole
Salmonella chemotactic response
cells
strong
chemo-
attraction
diffuse
chemo-
attraction
chemo-
halation
diffuse
chemo-
halation
strong
chemo-
repulsion
Salmonella growth versus L-Ser:indole ratio
1
0.5
0
relative growth
10:1
1:1
1:10
presumed
physiological range
5
mM
colitis
incubation
early infection